MICROCOPY RESOLUTION TEST CHART

NATIONAL BUREAU OF STANDARDS

⑦

# INSTITUTE FOR COMPUTATIONAL
# MATHEMATICS AND APPLICATIONS

Technical Report ICMA-86-102          November 1986

On the Computation of Multi-dimensional Solution
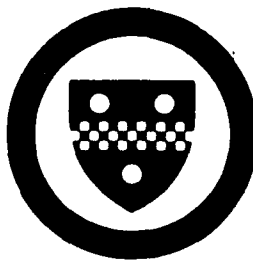
Manifolds of Parametrized Equations[1]

# Department of Mathematics and Statistics
# University of Pittsburgh

7

Technical Report ICMA-86-102          November 1986

On the Computation of Multi-dimensional Solution

Manifolds of Parametrized Equations[1]

by

Werner C. Rheinboldt

Institute of Computational Mathematics and Applications
Department of Mathematics and Statistics
University of Pittsburgh
Pittsburgh, PA  15260

DTIC

S ELECTE D

FEB 0 4 1987

E

# On the Computation of Multi-dimensional Solution Manifolds of Parametrized Equations [1]

by

Werner C. Rheinboldt [2]

Dedicated to Professor Ivo Babuska at his Sixtieth Birthday

**Abstract:** A new algorithm is presented for computing vertices of a simplicial triangulation of the p-dimensional solution manifold of a parametrized equation $F(x) = 0$, where F is a nonlinear mapping from $R^n$ to $R^m$, $p=n-m>1$. An essential part of the method is a constructive algorithm for computing moving frames on the manifold; that is, of orthonormal bases of the tangent spaces that vary smoothly with their points of contact. The triangulation algorithm uses these bases, together with a chord form of the Gauss-Newton process as corrector, to compute the desired vertices. The Jacobian matrix of the mapping is not required at all the vertices but only at the centers of certain local "triangulation patches". Several numerical examples show that the method is very efficient in computing triangulations, even around singularities such as limit points and bifurcation points. This opens up new possibilities for determining the form and special features of such solution manifolds.

# 1 Introduction

Parameter-dependent nonlinear equations

$$F(z, \lambda) = 0, \tag{1.1}$$

involving a state variable $z$ and a parameter vector $\lambda$, arise in many applications. Under natural conditions on $F$ and the relevant spaces the set of solutions $(z, \lambda)$ of (1.1) constitutes a differentiable manifold in the product of the state and parameter space, and the dimension of this manifold equals the parameter dimension.

In most practical applications interest centers not so much on computing a few *solutions of (1.1), but rather on determining the form and special features of the* solution manifold. For instance, if (1.1) represents an equilibrium problem, then we may wish to determine the bifurcation diagram or the boundaries of the stability regions on the manifold. But, as it turns out, all standard computational methods for such an analysis require us to construct a picture of a p-dimensional manifold from information along one-dimensional paths. In fact, all these methods belong to the family of continuation processes for which the dimension of the parameter space always has to equal one. Thus, before such a process can be applied, any problem with a larger parameter dimension must be reduced to some form involving only a scalar valued parameter and, geometrically, such a reduction is equivalent with a restriction to some path on the solution manifold of the original equation. A continuation method then computes a sequence of points along such a path. For example, in structural engineering the parameter $\lambda$ often characterizes a vector of load components in which case it has become customary to fix a linear combination of these components

specifying a particular load direction. The resulting reduced equation then involves
only the load intensity as a one-dimensional parameter variable and the standard
'incremental' methods generate points along this load path.

In general, it is not easy to develop a good picture of a p-dimensional manifold from
information along one-dimensional paths. Thus it is not surprising that there is growing
interest in computational methods which generate multi-dimensional grids of solution
points covering an entire segment of the manifold. Up to now the only method for
computing such multi-dimensional grids appears to be that of E.L.Allgower and
P.H.Schmidt [2]. It utilizes a simplicial continuation algorithm to "triangulate", by means
of p-simplices, a portion of a p-dimensional manifold defined by an equation of the
form (1.1).

Here we present a different method for computing vertices of such a triangulation of
segments of the p-dimensional solution manifold of an equation (1.1). An essential
part is a constructive algorithm for computing orthonormal moving frames on the
manifold in the sense first considered by E.Cartan; that is, of orthonormal bases of the
tangent manifolds that vary continuously with their points of contact (see e.g., [17]).
The resulting triangulation algorithm uses these bases and a predictor-corrector
approach to compute the desired grid points. Its has many similarities with the
continuation methods including a comparable computational complexity. In particular,
the Jacobian matrix of the mapping is not required at all the points. For example, on a
two-dimensional manifold the computation of a typical triangulation pattern with 114
triangles requires only 19 Jacobian decompositions.

After summarizing some basic concepts in Section 2 we introduce the moving frame

algorithm in Section 3. Then Section 4 outlines the general triangulation method and Section 5 presents several numerical examples. Finally, we end with an outlook on the utilization of the computed triangulations for the determination of specific features of the manifold.

## 2. Basic Concepts

Throughout this article, let

$$F: S \to R^m, \quad S \text{ open in } R^n, \quad p = n-m > 1, \tag{2.1}$$

be a differentiable mapping of class $C^r$, $r > 1$, on the subset S. As usual, a point $x \in S$ is called regular if the first derivative, $DF(x)$, of F has full rank m and hence maps $R^n$ onto $R^m$. We consider the equation

$$F(x) = 0 \ , \ x \in S, \tag{2.2}$$

and assume that its regular solution set

$$M = \{ x \in S \ ; \ F(x) = 0, \ x \text{ regular} \} \tag{2.3}$$

is non-empty. It is well-known that M is a p-dimensional $C^r$-manifold in $R^n$ without boundary (see, e.g., [17] or [15]).

The tangent space $T_x M$ at any point $x \in M$ may be identified with the kernel of the Jacobian $DF(x)$; that is,

$$T_x M = \ker DF(x) = \{ u \in R^n \ ; \ DF(x)u = 0 \}. \tag{2.4}$$

The normal space $N_x M$ at $x \in M$ is the orthogonal complement of the tangent space

under the natural Euclidean inner product on $R^n$; that is,

$$N_xM = (T_xM)^\perp = (\ker DF(x))^\perp = \mathrm{rge}\ DF(x)^T \qquad (2.5)$$

Since $DF(x)$ has maximal rank in some open subset $S_0$ of $S$ containing $M$, the mapping

$$x \in S_0 \rightarrow DF(x)^T[DF(x)DF(x)^T]^{-1}DF(x) \in L(R^n) \qquad (2.6)$$

from $S_0$ into the space $L(R^n)$ of all linear isomorphisms on $R^n$ is of class $C^{r-1}$ on $S_0$. Hence, the orthogonal projection

$$P: M \rightarrow L(R^n); \quad P(x) = I_n - DF(x)^T [DF(x)DF(x)^T]^{-1} DF(x), \ x \in M \qquad (2.7)$$

of $R^n$ onto $T_xM$ is a mapping of class $C^{r-1}$ on the manifold $M$, (here $I_n$ denotes the identity on $R^n$).

For the computation we require local coordinate systems on $M$. Any p-dimensional subspace $T$ of $R^n$ induces a local coordinate system of $M$ at any point $x \in M$ where

$$T \cap N_xM = \{0\}, \qquad (2.8)$$

In fact, if (2.8) holds for $x \in M$ then there exist open neighborhoods $Y_1$ and $Y_2$ of the origins of $T$ and $R^n$, respectively, as well as a unique $C^{r-1}$ function $w: Y_1 \rightarrow T^\perp$ with $w(0) = 0$, such that

$$M \cap Y_2 = \{ y \in R^n ; \; y = x + t + w(t), \; t \in Y_1 \}, \tag{2.9}$$

(see, e.g., [9] or [15]). In other words, in the local coordinate system induced by $T$, the point $y = x + t + w(t)$ of $M$ has the coordinate $t \in T$.

A point $x \in M$ where (2.8) holds is a non-singular point with respect to the given coordinate space $T$, else we call $x$ a singular point. Clearly, at any point $x \in M$ the tangent space $T_x M$ can be chosen as coordinate space and $x$ is non-singular with respect to it. In most applications, a "natural" parameter space $\Lambda$ is given, as indicated by the form of the equation (1.1), and the orthogonal subspace $Z = \Lambda^\perp$ is the state space. Then interest centers on determining the singular points with respect to the space $\Lambda$. These are the so-called foldpoints on $M$ where the tangent space has a non-zero intersection with the state space $Z$ and the parameter space $\Lambda$ can no longer be used as a local coordinate space. These are also the points where, for example, in equilibrium problems a change in the stability behavior of the physical system under study may be expected.

Numerically, the mapping $w$ of (2.9) can be implemented in various ways. A simple approach is based on a chord form of the Gauss-Newton method. At the given point $x \in M$ we compute the QR-factorization

$$DF(x)^T = Q \begin{bmatrix} R \\ 0 \end{bmatrix} \tag{2.10}$$

of the transposed Jacobian $DF(x)^T$ involving the $n \times n$ orthogonal matrix $Q$ and $m \times m$

nonsingular, upper triangular matrix $R$. Then, starting from any point $y$ in a suitable neighborhood of $x$ in $x + T_xM$, we may apply the process

1) Set $y^0 = y$;

2) for $k = 0, 1, \ldots$ until convergence $\qquad\qquad$ (2.11)

  2a) solve $R^T z = F(y^k)$ for $z \in R^p$;

  2b) compute the next iterate $y^{k+1} = y^k - Q(z, 0)^T$;

With (2.10) this is readily rewritten in the form

$$DF(x)(y^{k+1} - y^k) + F(y^k) = 0 , \quad y^{k+1} - y^k \in [\ker DF(x)]^{\perp} , \ k = 0, 1, \ldots \qquad (2.12)$$

which shows that $y^{k+1} - y^k \in N_xM$. Thus we have $y^k \in y + N_xM$ for all $k > 0$, whence the limit point $y^*$ -- if it exists -- is the unique point in the intersection of $M$ and $y + N_xM$ which, in the notation of (2.9), can be written as $y^* = x + t + w(t)$, $t = y - x$.

The convergence theory of Gauss-Newton processes is well understood. Earlier studies of these methods considered applications to least squares problems and hence assumed that $F$ maps $R^n$ into $R^m$ where $n < m$. A local convergence result which covers our case $n > m$ may be found in [8, Theorem 4]. Another simple proof for the method in the form (2.12) also follows along the lines of the convergence proof for singular chord methods given in [14]. These results guarantee the validity of the following theorem:

<u>Theorem 1</u>: Under the stated assumptions about the mapping $F$ there exists for any

point x of M a neighborhood $Y(x)$ of x in $x+T_xM$ such that for any starting point y in $Y(x)$ the Gauss-Newton process (2.11) converges to the unique point $y^*$ in the intersection of M and $y+N_xM$ that has the coordinate $t = y-x$ in the local coordinate system induced by the tangent space $T_xM$.

## 3. A Moving Frame Algorithm

As usual, a vector field of class $C^S$, $s \leq r$, on an open subset $M_0$ of our manifold $M$ is a $C^S$ function $u: M_0 \to TM$ from $M_0$ into the tangent bundle $TM$ such that $u(x) \in T_x M$ for all $x \in M_0$. A moving frame of class $C^S$ on $M_0$ is a mapping which associates with each $x \in M_0$ a frame (i.e., ordered basis) $\{u^1, ..., u^p\}$ of $T_x M$ such the functions $u^i: M_0 \to TM$, $i=1,...,p$, form $p$ vector fields of class $C^S$ on $M_0$. When such a moving frame exists on $M_0$ then the sub-manifold $M_0$ is said to be parallelizable. We will consider only orthonormal moving frames; that is, frames for which the basis vectors are orthonormal. (For a discussion of these concepts see, e.g., [17].)

Clearly, the problem of computing an orthonormal basis of the tangent space $T_x M$ of $M$ at a given point $x \in M$ is equivalent with the construction of an $n \times p$ matrix $U$ with orthonormal columns for which

$$DF(x)U = 0 \qquad (3.1)$$

There are many techniques for computing such a matrix. A well-known procedure is provided by the QR-decomposition (2.10). In fact, if the matrix $Q$ is partioned in the form $Q = (Q_1, Q_2)$ where $Q_1$ has m columns then we may use $U = Q_2$ as the desired basis. Various other techniques for computing $U$ have been proposed. We mention, in particular, the methods in [5] and [6] aimed at producing sparse bases $U$.

An algorithm for constructing a moving frame of class $C^S$ on some open subset $M_0$ of $M$ has to generate a basis matrix $U = U(x)$ for each $x \in M_0$ in such a way that the

mapping $U: M_0 \to L(R^p, R^n)$ is of class $C^s$. As T.F.Coleman and D.C. Sorensen [7] have noted, the approach based on the QR-decomposition does not give continuously varying matrices $U(x)$. This observation extends to other algorithms of a similar nature; in fact, it relates directly to the corresponding problems of computing eigenvectors associated with a multiple eigenvalue. Three remedies are proposed in [7], but they concern only the construction of a limit $U_0$ of a sequence of bases $U(x)$ when $x$ tends to $x_0$.

For our construction of a moving frame we restrict attention to open subsets $M_0$ of M where a given p-dimensional subspace T of $R^n$ induces a local coordinate system; that is, where (2.8) holds for all x of $M_0$. With a mild abuse of language, let $T_0$ be a p x p matrix with orthonormal columns which span the coordinate space T. Moreover, assume that we have picked some method for computing at any point x of $M_0$ an n x p matrix $U(x)$ with orthonormal columns that span the tangent space $T_x M$ at x. Of course, U is not expected to depend continuously on x. For instance, we may use the matrices produced by the QR-decomposition technique. For any orthogonal p x p matrix $Q = Q(x)$ the matrix $U(x)Q$ is another orthonormal basis of $T_x M$ and our aim is to construct matrices $Q(x)$ such that the "rotated" bases $U(x)Q(x)$ depend continuously on x for all x in $M_0$.

The normalization $(T_0)^T T_0 = I_p$ suggests that we choose the orthogonal matrix Q so that $(U(x)Q)^T T_0$ approximates the identity $I_p$. Various norms may be used for this, an advantageous choice is the Frobenius norm $\| A \|_F = [ \operatorname{tr}(A^T A) ]^{1/2}$. The resulting optimization problem

$$\| (U(x)Q)^T T_0 - I_p \|_F = \min, \text{ subject to } Q^T Q = I_p \tag{3.2}$$

is a case of the orthogonal Procustes problem. As discussed in [12], the following algorithm solves (3.2):

(1) $U_0 := U(x)^T T_0$;

(2) compute the singular value decomposition $\qquad\qquad (3.3)$

$\quad A^T U_0 B = \Sigma$ and save A and B;

(3) $Q := AB^T$.

For our purposes the essential fact is now the content of the following theorem.

<u>Theorem 2</u>: Let $M_0$ be an open subset of M on which the given p-dimensional subspace T of $R^n$ induces a local coordinate system. For any $x \in M_0$, let U(x) be an orthonormal basis matrix of $T_x M$ and compute the orthogonal matrix $Q = Q(x)$ of (3.3). Then the mapping $x \in M_0 \rightarrow U(x)Q(x) \in L(R^p,R^n)$ is of class $C^{r-1}$ on $M_0$ and defines an orthonormal moving frame on $M_0$.

<u>Proof</u>: Evidently, $U_0 z = 0$ implies that the tangent vector $U(x)z \in T_x M$ must be orthogonal to the subspace T of $R^n$ spanned by the columns of $T_0$, and, and hence that $U(x)z \in W$. By construction of $M_0$ this cannot happen for $x \in M_0$ unless $z = 0$. In other words, for $x \in M_0$ the matrices $U_0$ and $\Sigma$ arising in (3.3) are non-singular. Now

$$U_0 = A\Sigma B^T = AB^T(B^T I B) = QH, \quad H = B^T \Sigma B.$$

is the polar decomposition of $U_O$ and it follows that

$$H = [(U_O)^T U_O]^{1/2} = [(T_O)^T U(x) U(x)^T T_O]^{1/2}$$

is non-singular, whence

$$Q = (U_O)^T T_O [(T_O)^T U(x) U(x)^T T_O]^{-1/2}.$$

Evidently, $U(x)U(x)^T = P(x)$ is the orthogonal projection (2.7) from $R^n$ onto $T_x M$. Thus we see that

$$U(x)Q = P(x)T_O [(T_O)^T P(x) T_O]^{-1/2} \qquad (3.4)$$

and, since P was already shown to be of class $C^{r-1}$ on M, the result follows.

Our overall moving frame algorithm on $M_O$ now consists of the following three steps:

(1) Given $x \in M_O$, compute the basis matrix $U(x)$ of $T_x M$;

(2) compute the orthogonal matrix Q by (3.3); $\qquad (3.5)$

(3) form the desired basis matrix $U(x)Q$.

If the QR-factorization is used in step (1), then the order of the number of floating point operations required is as follows:

| | |
|---|---|
| Computation of $U(x)$ | $O(nm^2)$ |
| Multiplication $U(x)^T T_O$ | $O(np^2)$ |

$$\text{Singular value decomposition} \qquad O(p^3)$$
$$\text{Formation of the product } U(x)\Omega \qquad O((n+p)p^2)$$

Thus, when the dimension p of the manifold is small in comparison with the space-dimension n, as is typical in applications, then the principal cost is related to the QR-factorization of $DF(x)^T$ and involves about $(2/3)n^3$ operations. This is indeed analogous to the complexity of a standard continuation process.

For the practical implementation it is certainly desirable to choose the basis matrix $T_0$ of our reference coordinate space T in $R^n$ as simply as possible. In particular, it is very advantageous to define T as a subspace spanned by p appropriate natural basis vectors $e^1,...,e^n$ of $R^n$. Then $T_0$ can be taken as a matrix with columns $e^i$ with certain distinct indices $i=i_j$, $1 \le i_j \le n$, $j=1,...,p$. For the choice of these indices, recall that for any x of M and given vector $a \in R^n$ the principal angle $\alpha \in [0,\pi/2]$ between $T_xM$ and span{a} is defined by

$$\cos(\alpha) = \max\{\, u^T a \; ; u \in T_xM, \|u\|_2 = 1 \,\}$$

Evidently, if a is one of the global basis vectors of $R^n$, then

$$\cos(\alpha_i) = \|U(x)^T e^i\|_2, \quad i=1,...n; \qquad (3.6)$$

that is, the Euclidean norm of the i-th row of U(x) is the cosine of the principal angle between the tangent space $T_xM$ and the i-th coordinate line span{$e^i$} of $R^n$. Since the Euclidean norm is invariant under orthogonal transformations, it is obvious that the principal angle does not depend on the particular basis U(x) of $T_xM$.

This suggests the desired selection of $T_0$. We initialize our moving frame algorithm at some reference point $x^*$ of M and compute a basis matrix $U(x^*)$ of the tangent space of M at this point. This allows for a straightforward calculation of the principal direction cosines $\tau_i = \cos(\alpha_i)$ of (3.6) which we order in descending order of size. Let $i_1,...,i_p$ be the indices of the p largest of these $\tau_i$ (with ties broken, say, by lexicographic ordering), then the corresponding natural basis vectors of $R^n$ span our reference coordinate space T and form the columns of the basis matrix $T_0$. Since $U(x^*)$ has rank p, none of the selected coordinate directions can be orthogonal to the tangent space. Hence, as required, $x^*$ is a non-singular point with respect to T, and the subset $M_0$ of Theorem 1 contains an open neighborhood of $x^*$ on M. Geometrically the constructed subspace T is close to the tangent space of M at $x^*$ in the sense of the above maximization of the direction cosines (3.6). In fact, our construction is analogous to the local coordinate selection used in the continuation program PITCON (see [15] or [16]). Obviously, this choice of $T_0$ also has the advantage that the computation of the matrix $U_0$ in step (1) of the algorithm (3.3) simply becomes an extraction of p of the rows of $U(x)$.

A frequently occurring case are manifolds with dimension $p = 2$. For them we can compute, up to signs, a direct representation of the orthogonal matrix Q of the algorithm (3.3). In fact, suppose that

$$U_0 = \begin{bmatrix} a & b \\ c & d \end{bmatrix}$$

is the matrix in step (1) of (3.3). Then a straightforward calculation shows that

$$Q = \begin{bmatrix} \tau & -\sigma \\ \sigma & \tau \end{bmatrix}$$

with

$$\tau = \pm (a + d)/\delta, \quad \sigma = \pm (b - c)/\delta, \quad \delta = [(a+d)^2 + (b-c)^2]^{1/2}.$$

The signs are readily chosen by comparing the directions of the computed frame with the directions of the natural basis vectors used in $T_0$. This leads also to a direct proof of the theorem in this special case.

## 4. A Triangulation Algorithm

The results of the previous section are now used to generate the desired triangulation on a subset of our manifold M. The basic idea is as follows: We introduce a reference triangulation on $R^p$ and use the bases produced by the moving frame algorithm to map segments of it onto the spaces $x+T_xM$ corresponding to appropriate points $x$ on M. Then the Gauss-Newton process (2.11) is applied to "project" these triangulations from $x+T_xM$ onto M.

The reference triangulation, of course, is any covering of $R^p$ by a locally finite collection of p-simplices such that any two of these simplices intersect either in a common face or not at all. The literature on this topic is large and we refer here only to the discussion of various numerically efficient triangulations in [18]. Our algorithm does not place any particular restrictions on the choice of this triangulation except that we should be guided by considerations of computational simplicity. Let $\Sigma$ be the collection of simplices of this triangulation.

Most triangulations used in simplicial continuation studies are generated by pivoting rules. A simple such rule is pivoting by reflection. For any index $j \in \{1,2,...,p\}$ set $j_+ = j+1$ and $j_- = j-1$ with the provision that $j_+ = 1$ if $j = p$ and $j_- = p$ if $j = 1$. Then, for a given p-simplex $\sigma = [y^0, y^1, ..., y^p]$ in $R^p$, pivoting by reflection of the vertex $y^j$ is defined as the replacement of $\sigma$ by the simplex $[y^0, ..., y^{j-1}, y^{j_+}+y^{j_-}-y^j, y^{j+1}, ..., y^p]$. If $\sigma_0$ is a given reference simplex in $R^p$, then by repeated application of this procedure a triangulation of $R^p$ can be generated (see, e.g. [1]).

A frequently used example is the so-called Kuhn triangulation which is generated by repeated pivoting by reflection starting with the simplex

$$\sigma_0 = [ 0, e^1, e^1 + e^2, ..., e^1 + e^2 + ... + e^p ].$$

In the often occuring case $p = 2$, we can also use triangulations of $R^2$ by equilateral triangles generated by pivoting by reflection beginning with the 2-simplex

$$\sigma_0 = [ 0, e^1, 0.5(e^1 + \sqrt{3} e^2) ]. \qquad (4.1)$$

Let $\xi$ denote a given vertex of the triangulation in $R^p$ and $\delta > 0$ a fixed steplength. Then for any point $x \in M$ where a basis matrix $U$ of $T_x M$ is known, the mapping

$$A : R^p \rightarrow x + T_x M , \quad A\eta = x + \delta U(\eta-\xi), \quad \eta \in R^p \qquad (4.2)$$

transfers $\Sigma$ onto $x + T_x M$. As in Theorem 1, let $Y(x)$ denote the local convergence domain in $x + T_x M$ of the Gauss-Newton process (2.11). If $\eta$ is a vertex of $\Sigma$ for which $A\eta$ belongs to $Y(x)$, then (2.11) can be used to map $A\eta$ into a point $y \in M$. The set $\Gamma(\xi,x,U,\delta)$ of vertices of $\Sigma$ that can be mapped onto M in this way shall be called the "patch" corresponding to the information $\xi,x,U,\delta$.

An idealized version of our algorithm can now be formulated as follows:

(1) Select a reference vertex $\xi = \xi^*$ of $\Sigma$ ;

(2) select a reference point $x = x^*$ of M ;

(3) initialize the moving frame algorithm at $x^*$ and let $M_0$ be the

subset where, by Theorem 2, this algorithm applies;

(4) mark the vertex $\xi$ as used; (4.3)

(5) while x belongs to $M_0$

(5a) mark $\xi$ as a "center";

(5b) compute the frame $U = U(x)$ by the moving frame algorithm;

(5c) select all vertices of the patch $\Gamma(\xi,x,U,\delta)$ which have

not yet been marked "used";

(5d) use (4.2) to map these vertices onto $x+T_xM$ and mark them "used";

(5d) use the Gauss-Newton process to project the resulting points

from $x+T_xM$ onto M;

(5e) choose a "used" vertex $\xi$ of $\Sigma$ not marked a "center"

and let x be its computed image on M;


The points computed on M inherit the connectivity pattern of the original simplices of

$\Sigma$ which in turn induces a simplicial approximation $M_\Sigma$ of a segment of M in $R^n$. The

algorithm is still "ideal" in nature since, in practice, the sets $M_0$ and $\Gamma(\xi,x,U,\delta)$ are not

known explicitly. Without this knowledge the computation may halt when the iteration

in step (5d) fails to converge; that is, when we encounter a point in the affine space

$x+T_xM$ of one of the centers x which does not belong to the neighborhood $V(x)$

specified in Theorem 2. A second possibility for failure arises in the execution of the

moving frame algorithm in step (5b) when the selected center x does not belong to $M_0$


In order to make the algorithm practical, we replace the "ideal" patches $\Gamma(\xi,x,U,\delta)$ in

step (5c) by "standardized" patches $\Gamma_0(\xi)$. The definition of these patches depends on

the specific reference triangulation in $R^p$. As an example, consider the earlier

mentioned triangulation on $R^2$ consisting of equilateral triangles produced by pivoting

by reflection from the triangle (4.1). Then the standarized patch for the center point

(0,0) in Figure 1 is the hatched, star-shaped region and for any other vertex it is

obtained by obvious translation. With this standard patch the progress of the algorithm

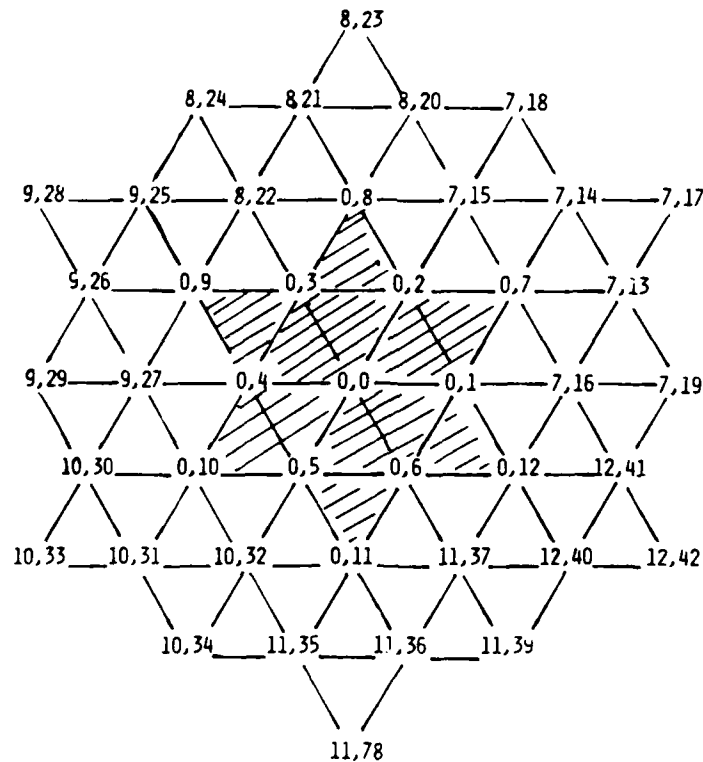is easily folllowed in Figure 1. There, at each vertex, the second of the two integers is a



Figure 1

counter and the first one identifies the "center" $\xi$ that is used in mapping that vertex onto M. Thus after the initial vertex 0, the nodes 7,...,12 become centers which serve to map the nodes 13,...,42 onto M. Then the process continues with nodes 17, 18, 19, 23, 24, 28, 29, 33, 34, 38, 39, 42 as centers. This is no longer shown *in the figure*, but, in practice, we have always continued through this further stage. It results in the earlier mentioned total of 114 triangles involving 19 centers and hence as many Jacobian evaluations.

Once a standarized patch $\Gamma_0(\xi)$ is used in step (5c), a suitable divergence check has to be built into the Gauss-Newton process. If in step (5d) this check is triggered, then the corresponding vertex $\xi$ of $\Sigma$ is flagged as unusable. Such unusable vertices are excluded from the further computation. A similar procedure may be followed when in step (5b) the moving frame algorithm fails. However, in the latter case it is often *advantageous to re-initialize the moving frame algorithm at one of the successfully computed points x on M*. Of course, then the computed basis U(x) has to be used as the reference matrix $T_0$.

The above provisions may result in triangulations that cover a somewhat irregular domain on M. Fortunately, in practice, this does not occur as frequently as might be expected, provided the steplength $\delta$ is not chosen too large. Alternately, it is natural to consider a procedure which adapts $\delta$ in cases of failures and hence which produces irregular triangulations on M. Such a program is now being implemented.

## 5. Numerical Experiments

In this Section we present results of some numerical experiments with the triangulation algorithm. The method produces a wealth of numerical data which cannot be reproduced in the limited space of this paper. At the same time, it is a challenging problem to invent instructive graphical representations of manifolds of dimension larger than 2. As a consequence, only some graphical results for two-dimensional manifolds are shown here. It is hoped that other experiments with higher dimensional manifolds can be presented elsewhere.

**An Exotherm. Reaction:** As a first example we consider a simple transport model for an exothermic, first-order reaction-scheme discussed in [4] which, in dimensionless form, leads to a two-point boundary value problem

$$(Du')' + k_0 (\mu - u) \exp(-\lambda (1+u)^{-1}) = 0, \quad u(0) = u(L) = 0. \tag{5.1}$$

The dimensionless parameters $\mu$ and $\lambda$ involve the constant concentration and temperature on the outside of the system, and for the calculation we follow [4] and set $D = 1$, $L = 1$, and $k_0 = 10^7$. The standard finite difference approximation of (5.1) on a uniform mesh $x_i = ih$, $i = 0,1,...,n+1$, $h = (n+1)^{-1}$ then produces a nonlinear equation of the form

$$-x_{i-1} + 2x_i - x_{i+1} = h^2 k_0(\mu - x_i)\exp(-\lambda(1+x_i)^{-1}), \ i=1,...,n, \ x_0 = x_{n+1} = 0 \tag{5.2}$$

For $\mu = 1$ there is a simple turning in $\lambda$ near $\lambda = 22$ which was calculated with the continuation code PITCON and n=10. This point was then used to initialize the

triangulation algorithm. Here -- as in the subsequent example -- the reference

triangulation in $R^2$ was generated by repeated pivoting by reflection from the

equilateral triangle (4.4). The stepsize in the affine mapping (4.5) was $\delta = 0.4$. Figure 2

shows the results of this triangulation. More specifically, the intersection of the

computed simplicial approximation $M_\Sigma$ with the $(\lambda, \mu, x_c)$-space is shown, where $x_c$ is

the computed x-value at the center of the interval. The coordinate axes are slightly

rotated and one see clearly the starshaped pattern of the reference triangulation of

Figure 1 as it was mapped onto the manifold. The floor of the valley actually

represents a foldline as can be seen in Figure 3, where the same surface in $(\lambda, \mu, x_c)$-

space is projected onto the $(\lambda, \mu)$-parameter plane. It shows also that the location of

the turning point in $\lambda$ depends approximately linearly on $\mu$.


A Shallow Circular Arch: As the second example we consider a finite-element model

for the deformation of a thin, shallow, circular arch which has been used as a test case

by many authors. It appears to go back to A.C. Walker [19] and we employ here the

same formulation as in [13]. In particular, in a $(r,\Theta)$-polar coordinate system with the

vertical direction as the r-axis, the unloaded configuration of the arch is represented by

the circular segment $\{(r,\Theta) ; r = 10, -\Theta_0 \leq \Theta \leq \Theta_0, \Theta_0 = 15^\circ\}$ and , for pinned ends,

the dimensionless total potential energy and associated boundary conditions are given

by

$$\int_{-\Theta_0}^{\Theta_0} \left[ \left[ (w'-u) + \alpha_0 (u')^2 \right]^2 + \alpha_1 (u'')^2 - \alpha_2 p u \right] d\Theta \ , \ u(\Theta)=w(\Theta)=u''(\Theta)=0, \ \Theta=\pm\Theta_0$$

where primes denote derivatives with respect to $\Theta$. For the asymmetrical load

$$p(\Theta) = (1-\mu)\lambda, \text{ if } -\Theta_0 \le \Theta < 0, \text{ and } p(\Theta) = (1+\mu)\lambda, \text{ if } 0 \le \Theta \le \Theta_0,$$

involving the two parameters $\mu$ and $\lambda$, the load path for $\mu = 0$ has a bifurcation point near $\lambda = 1.9$. This point was computed with PITCON and used to initialize the triangulation algorithm. The stepsize of the mapped triangles was $\delta = 0.5$. The results are shown in Figure 4. More specifically, let $x_c$ denote the (dimensionless) radial deformation at the center, then the figure shows the intersection of the manifold with the $(x_c, \lambda, \mu)$-space projected orthogonally onto the $(\lambda, \mu)$-plane. The cusp - bifurcation is clearly visible and the saddle shape of the surface can be seen even better in the slightly rotated Figure 5.

The problem was also run with the load function

$$p(\Theta) = \lambda[1-4(\mu-\Theta)(\Theta_0)^{-1}], \text{ if } \max(-\Theta_0, \mu-0.25\Theta_0) \le \Theta \le \mu,$$
$$p(\Theta) = \lambda[1+4(\mu-\Theta)(\Theta_0)^{-1}], \text{ if } \mu \le \Theta \le \min(\Theta_0, \mu+0.25\Theta_0),$$

considered already in [3]. In other words, the load is a piecewise-linear hat function which has the value $\lambda$ at $\Theta = \mu$ and is zero outside the interval centered at $\mu$ of width $0.5\Theta_0$.

Figures 6 and 7 give results with this load obtained at two initialization points. More specifically, the computations for these figures were centered at the limit points with respect to $\lambda$ when $\mu$ is fixed at $\mu=0$ or $\mu = 0.05$, respectively. Once again these limit points were computed with PITCON. The foldline in the $(\mu, \lambda)$-plane has the shape shown in Figure 8 and Figures 6 and 7 clearly show segments of this foldline. In

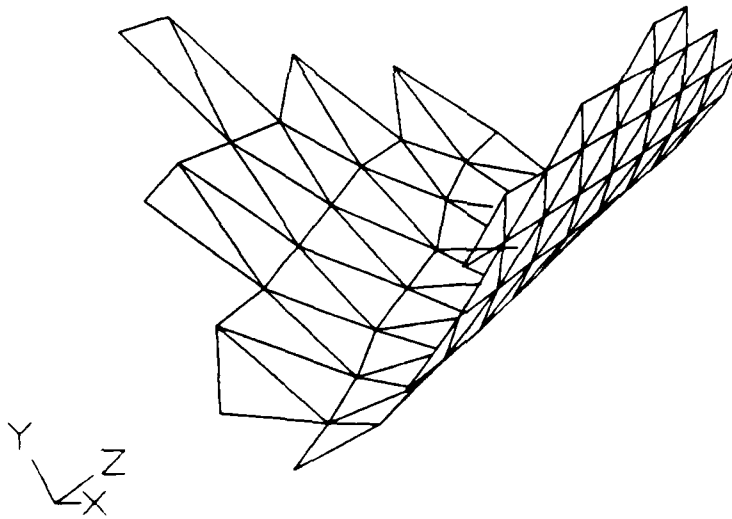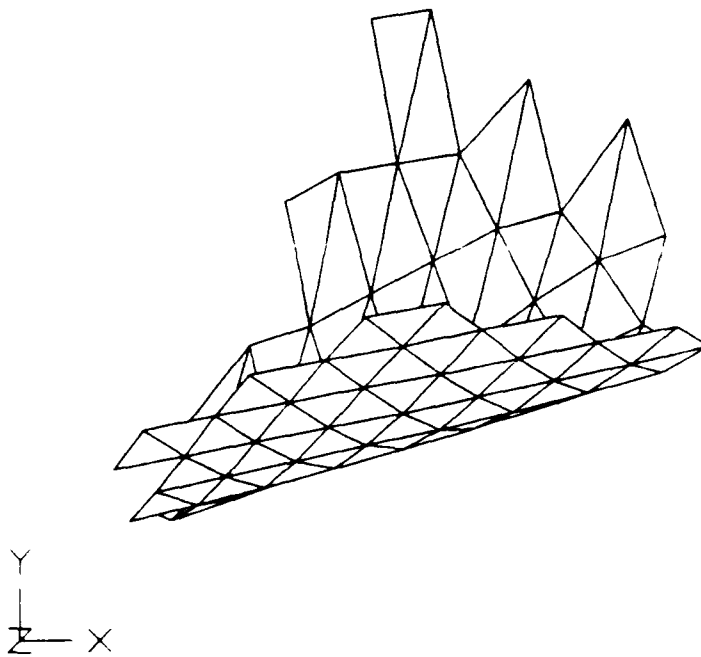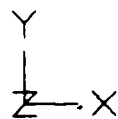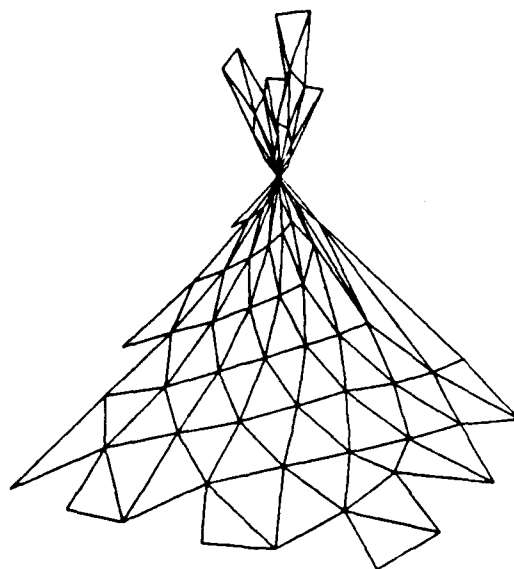particular, Figure 7 contains one of the points where the most dangerous load occurs, namely at about $\mu = 0.16\Theta_0$.



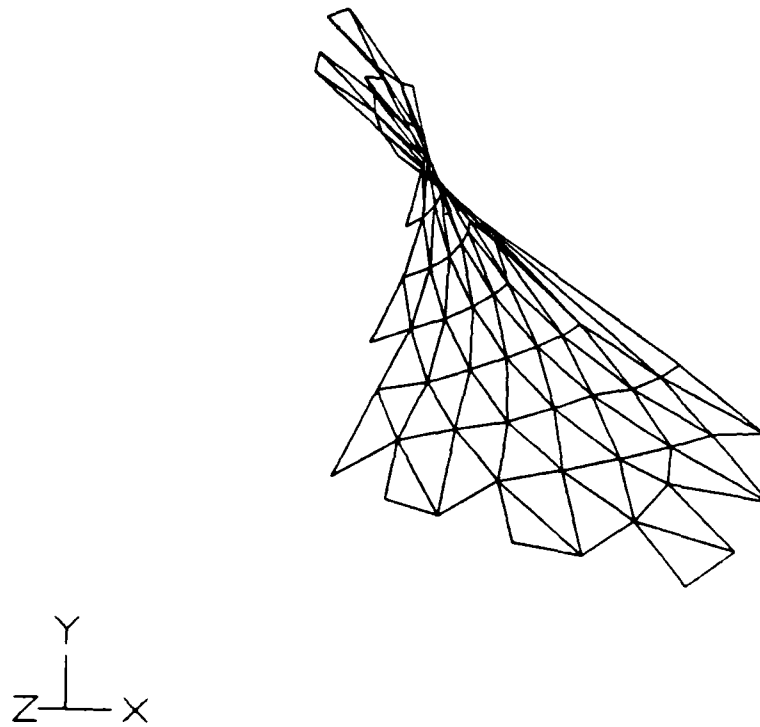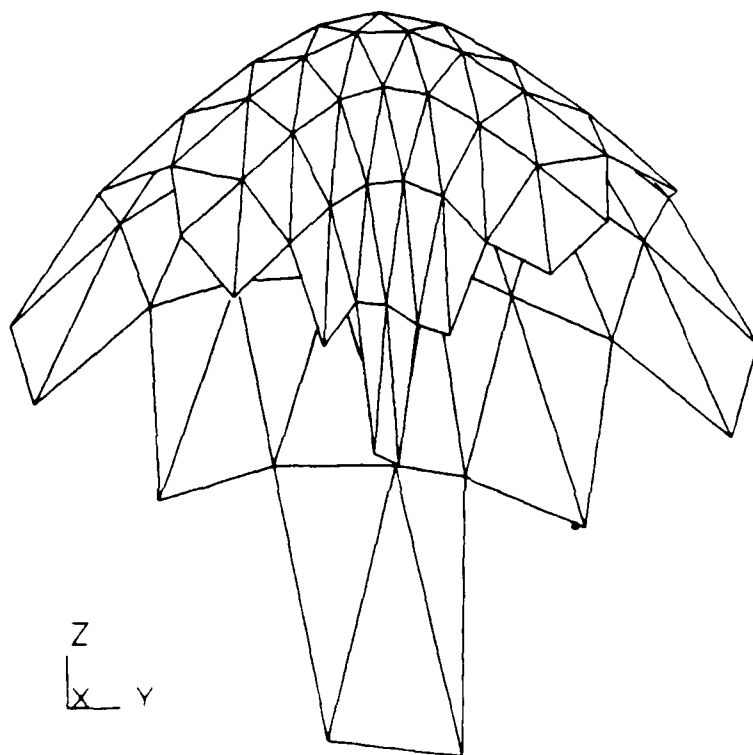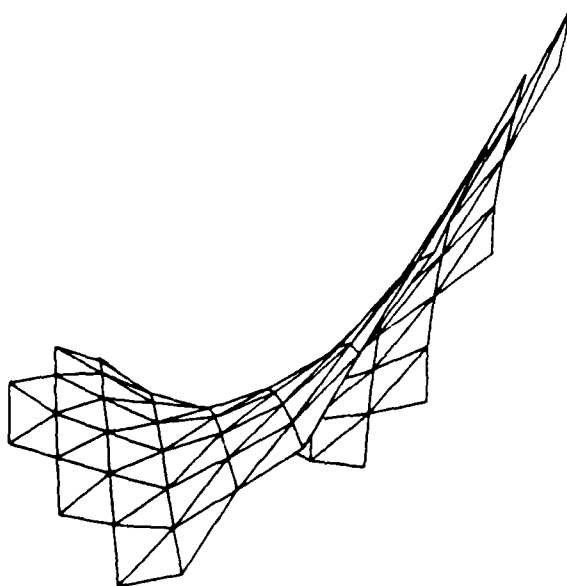Figure 2

Figure 3

Figure 4

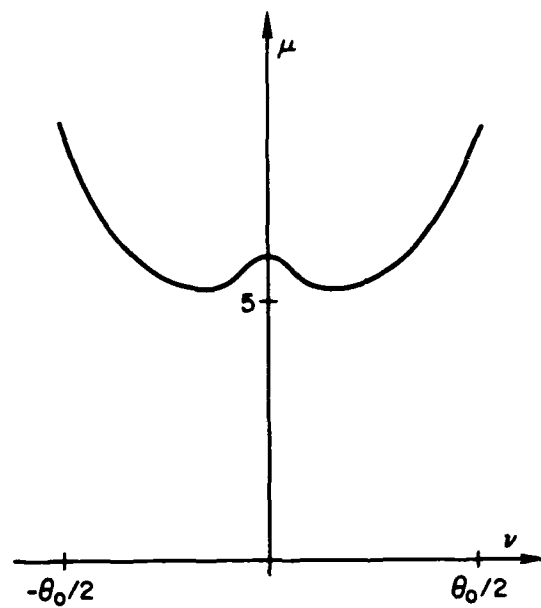Figure 5

Figure 6

Figure 7

Figure 8

## 6. Outlook

The numerical examples indicate that the triangulation algorithm works very efficiently even around singularities. Thus -- as intended -- it does indeed offer a new tool for deriving information about the shape and features of the manifold. Of course, as mentioned before, we are able to present here only some graphical information and none of the extensive numerical output of the algorithm. This output is available as input to various post-processes for extracting further information. Several such processes are now under development and will be described elsewhere in more detail. Here we present only a brief overview of some of the possibilities.

As noted earlier, linear interpolation between the vertices of the computed triangulation defines a simplicial approximation $M_\Sigma$ of the corresponding part of the manifold M. The points of $M_\Sigma$ can be used to compute further points of M. For example, we may project any such point onto M by applying the corrector iteration (2.11). Alternately, we can augment the system (2.2) with p appropriately chosen equations and then apply, say, a chord Newton method to calculate a corresponding point on M. This approach is useful when points on M with specific properties are desired. For example, we may be interested in certain target points where the parameters have prescribed values. In that case, these target conditions become the augmenting equations and we may start the iterative process from a point on $M_\Sigma$ where the parameters have the specified values. Augmenting equations are also essential when we are interested in determining the specific location of certain types of singularities. For the computation of limit points a comparison of various such augmentations was given in [13], and for higher order singularities the literature on suitable augmentations is fairly extensive. In our present setting, the "minimal" augmentations discussed in

[11], and thereafter in [10]), appear to be of particular interest.

For any given functional the computed data allow us to generate contour plots on the intersection of the simplicial approximation $M_\Sigma$ with various subspaces. For instance, in some structural problem we might be interested in seeing lines, where some stress component is constant, plotted in dependence of certain other variables. A special example of such a contour plot involves the graphical representation of lines of foldpoints. As the figures of the previous section already show, our triangulations provide information for approximating segments of such foldlines. One approach for detecting foldpoints is to monitor the orientation of the projection of the tangent basis onto the parameter space. If there is a change in this orientation then we have passed through a foldpoint, but the converse is not necessarily true; that is, not every foldpoint can be detected this way. The orientation is characterized by the determinant of the projected basis in the parameter space. Thus, if we plot lines of constant determinant values, then lines of zero determinant are approximations of the desired foldlines. Of course, for this we need the tangent basis at each vertex of the triangulation and that increases the cost of the overall algorithm. However, there appear to be other possible techniques for approximating foldlines from data obtained by our triangulation algorithm. This will not be pursued here.

Even though these contour plots only provide lines of constant values on the simplicial approximation $M_\Sigma$ rather than on M itself, they tend to offer already good insight into the shape of the manifold. Of course, as discussed earlier, we can always call on various local corrector methods to project these lines onto M itself.

So far we mentioned only the need for appropriate post-processing techniques

for analyzing the output of our triangulation method. There is also considerable room for improving the algorithm itself. In particular, for large sparse problems the QR-factorization may be computationally expensive. As noted earlier, there exist results for computing sparse bases of the null space of a matrix (cf [5], [6]). The rotation require ' for the moving frame algorithm is likely to destroy this sparsity, and hence the rotated basis should not be stored but computed only as needed. In the case of low dimensional manifolds, this is not very costly as long as the computation of the original basis of the tangent space takes account of the sparsity structure of the Jacobian.

# References

[1]   E.L. Allgower and K. Georg, Generation of Triangulations by Reflections; Utilitas
      Math., 16, 1979, 123-129

[2]   E.L. Allgower and P.H.Schmidt, An Algorithm for Piecewise-linear Approximation
      of an Implicitly Defined Manifold; SIAM J. Numer. Anal., 22,1985, 322-346

[3]   I.Babuska and W.C. Rheinboldt, Adaptive Finite Element Processes in Structural
      Mechanics; in Elliptic Problem Solvers II, ed. by C Birkhoff and A.Schoenstadt,
      Academic Press, Inc. 1984, pp 345-378

[4]   E. Bohl, Finite Modelle gewöhnlicher Randwertaufgaben, B.G.Teubner,
      Stuttgart, Germany 1981

[5]   M.W.Berry, M.T.Heath, I.Kaneko, M.Lawo, R.J.Plemmons, and R.C.Ward, An
      Algorithm to Compute a Sparse Basis of the Null Space; Numer. Math.
      47,1985,483-504

[6]   T.F. Coleman and A.Pothen, The Null Space Problem II: Algorithms, Cornell
      Univ., Dept. of Comp. Science, Techn. Rep. TR 86-747, April 1986

[7]   T.F.Coleman and D C. Sorensen, A Note on the Computation of an Orthonormal
      Basis for the Null Space of a Matrix; Mathem. Progr. 29,1984, 234-242

[8]   P. Deuflhard and G.Heindl, Affine Invariant Convergence Theorems for Newton's

Method and Extensions to Related Methods; SIAM J. Numer. Anal., 16, 1979,
1-10

[9]  J.P.Fink and W.C.Rheinboldt, Solution Manifolds of Parametrized Equations and
their Discretization Error; Numer. Math. 45,1984,323-343

[10]  J.P.Fink and W.C.Rheinboldt, A Geometric Framework for the Numerical Study of
Singular Points; University of Pittsburgh, Inst. f. Comput. Mathem. and Applic.,
Technical Report ICMA-86-90, January 1986; SIAM J. Num. Anal., in press.

[11]  A.Griewank and G.W.Reddien, Characterization and Computation of
Generalized Turning Points; SIAM J. Numer. Anal. 21,1984, 176-185

[12]  G.H. Golub and C. F. VanLoan, Matrix Computations;
The Johns Hopkins University Press, Baltimore, MD 1983

[13]  R.G.Melhem and W.C.Rheinboldt, A Comparison of Methods for Determining
Turning Points of Nonlinear Equations; Computing 29,1982,201-226

[14]  W.C.Rheinboldt, Numerical Methods for a Class of Finite-dimensional Bifurcation
Problems. SIAM J. Num. Anal., 17,1980, 221-237

[15]  W.C.Rheinboldt, Numerical Analysis of Parametrized Nonlinear Equations.
J. Wiley and Sons, Inc., New York, NY 1986

[16]  W.C.Rheinboldt and J.V.Burkardt, A Locally Parametrized Continuation Process,

ACM Trans. Math. Software, 9,1983, 236-246


[17]  M. Spivak, A Comprehensive Introduction to Differential Geometry;
Publish or Perish, Inc. Berkeley, CA, Five Volumes, Second Edition, 1979


[18]  M.J.Todd,  The Computation of Fixed Points and Applications;
Springer Verlag Inc.,  New York, NY  1976


[19]  A.C Walker,  A Non-Linear Finite Element Analysis of Shallow Circular Arches;
Int. J. for Solids and Struct. 5, 1969, 97-107

Encl (1)

| REPORT DOCUMENTATION PAGE | | READ INSTRUCTIONS BEFORE COMPLETING FORM |
|---|---|---|
| 1. REPORT NUMBER<br><br>ICMA-86-102 | 2. GOVT ACCESSION NO.<br><br>*ADA 176 586* | 3. RECIPIENT'S CATALOG NUMBER |
| 4. TITLE (and Subtitle)<br><br>On the Computation of Multi-dimensional Solution Manifolds of Parametrized Equations | | 5. TYPE OF REPORT & PERIOD COVERED |
| | | 6. PERFORMING ORG. REPORT NUMBER |
| 7. AUTHOR(s)<br><br>Werner C. Rheinboldt | | 8. CONTRACT OR GRANT NUMBER(s) |
| 9. PERFORMING ORGANIZATION NAME AND ADDRESS<br><br>Department of Mathematics & Statistics<br>University of Pittsburgh<br>Pittsburgh, PA 15260 | | 10. PROGRAM ELEMENT, PROJECT, TASK AREA & WORK UNIT NUMBERS |
| 11. CONTROLLING OFFICE NAME AND ADDRESS<br>Office of Naval Research<br>Mathematical Sciences Division<br>Arlington, VA 22217 | | 12. REPORT DATE<br>November 1986 |
| | | 13. NUMBER OF PAGES<br>37 |
| 14. MONITORING AGENCY NAME & ADDRESS(If different from Controlling Office) | | 15. SECURITY CLASS. (of this report)<br><br>Unclassified |
| | | 15a. DECLASSIFICATION/DOWNGRADING SCHEDULE |

16. DISTRIBUTION STATEMENT (of this Report)

Approved for public release: distribution unlimited

17. DISTRIBUTION STATEMENT (of the abstract entered in Block 20, if different from Report)

18. SUPPLEMENTARY NOTES

19. KEY WORDS (Continue on reverse side if necessary and identify by block number)

Parametrized Equation; Solution Manifold; Equilibrium Problem; Triangulation; Moving Frames

20. ABSTRACT (Continue on reverse side if necessary and identify by block number)

A new algorithm is presented for computing vertices of a simplicial triangulation of the p-dimensional solution manifold of a parametrized equation $F(x) = 0$, where $F$ is a nonlinear mapping from $R^n$ to $R^m$, $p = n-m \geq 1$. An essential part of the method is a constructive algorithm for computing moving frames on the manifold; that is, of orthonormal bases of the tangent spaces that vary smoothly with their points of contact. The triangulation algorithm

DD ₁ FORM 1473 EDITION OF 1 NOV 65 IS OBSOLETE
S N 0102-LF-014-6601

Unclassified

## 20. Abstract (continued)

uses these bases, together with a chord form of the Gauss-Newton process
as corrector, to compute the desired vertices.  The Jacobian matrix of the
mapping is not required at all the vertices but only at the centers of certain
local "triangulation patches".  Several numerical examples show that the
method is very efficient in computing triangulations, even around singularities
such as limit points and bifurcation points.  This opens up new possibilities
for determining the form and special features of such solution manifolds.

END
3-87
DTIC